JOURNAL OF CATALYSIS 150, 407–420 (1994)

Molybdena on Silica Catalysts: Role of Preparation Methods on the Structure–Selectivity Properties for the Oxidation of Methanol

Miguel A. Bañares, Hangchun Hu, and Israel E. Wachs[1]

Zettlemoyer Center for Surface Studies and Department of Chemical Engineering and Chemistry, Lehigh University, Bethlehem, Pennsylvania 18015

Received May 9, 1994; revised August 16, 1994

A series of MoO_3/SiO_2 samples prepared by several research groups, employing different silicas and preparation methods, have been studied by *in situ* Raman spectroscopy, X-ray photoelectron spectroscopy, and methanol oxidation as a probe reaction. The *in situ* Raman spectroscopy studies show that under dehydrated conditions the molecular structure of the silica-supported molybdenum oxide surface species is independent of the preparation methods used in the present study. The surface molybdenum oxide species is assigned to an isolated, highly distorted octahedral mono-oxo Mo structure. The appearance of new structures in some samples is due to the presence of calcium impurities in the silica supports which result in the formation of calcium molybdate. Neither the preparation method nor the specific silica used affected the methanol oxidation activity of the MoO_3/SiO_2 catalysts. The surface molybdenum oxide coverage on silica is the only relevant factor that determines the catalytic properties during methanol oxidation. *In siu* Raman spectroscopy during methanol oxidation shows aggregation of surface molybdenum oxide species to crystalline beta-MoO_3. The extent of aggregation increases with the surface molybdenum coverage, even at very low coverages, and accounts for the decrease in the methanol oxidation catalytic activity with increasing surface molybdenum coverage.

INTRODUCTION

Molybdena on silica catalysts are widely used in a number of reactions such as propene metathesis (1, 2), propene oxidation (3), methanol oxidation (4), ethanol oxidative dehydrogenation (1), and ammonia selective oxidation to nitrogen (5), and in the selective oxidation of methane (6, 7). These numerous catalytic applications have generated much interest in the structures of these catalysts and their relevance to their catalytic properties (1, 2, 8, 9). Furthermore, there has developed an interest in tailoring the structures of the surface molybdenum species to improve their catalytic properties for specific applications.

[1] To whom all correspondence should be addressed.

In the past few years, many authors have reported various structures or synthesis methods which are proposed to generate a specific surface molybdenum oxide species at low coverage: isolated dioxo surface MoO_4 species (4, 10), isolated mono-oxo MoO_6 species (5, 11), or dimeric surface Mo_2O_8 compounds (12) (See Scheme 1). Some synthesis methods have been reported to result in a better dispersion and catalytic activity than other preparation methods (4, 11, 12). Unfortunately, disagreements are quite frequently found in the literature in the structures obtained even when using the same preparation methods. Possible reasons for these discrepancies may be the use of different characterization techniques, conditions of characterization, or the presence of impurities in the catalysts.

The most common method employed to deposit molybdenum oxide on the silica support surface is by aqueous impregnation with ammonium heptamolybdate ($(NH_4)_6Mo_7O_{24} \cdot 4H_2O$) solutions (6, 7, 10, 11, 13). In this preparation method, the water solvent is removed by drying and the dry precursor is calcined at temperatures ranging from 723 to 873 K. At low Mo loadings and under dehydrated conditions, the dispersed surface molybdenum oxide species are reported to have either the hexacoordinated mono-oxo structure as concluded from Raman spectroscopy (11) or the tetracoordinated dioxo structure as concluded from luminescence (14, 15). Alternative synthesis methods have also been employed due to the poor effectiveness of this conventional impregnation method in producing samples with high dispersions of Mo. These new methods focused on an improvement of the interaction between the molybdenum oxide precursors and the silica surface hydroxyl groups by the use of molybdenum compounds with labile ligands (such as $MoCl_5$, $Mo(\eta^3C_3H_5)_4$, $Mo_2(\eta^3C_3H_5)_4$, or $Mo_2(OAc)_4$) that would be easily hydrolyzed by the silanol groups (11, 12, 15–18). Another approach is to improve the acid/base interaction of the molybdenum oxide precursor with the silica support by using the less acidic Mo^{3+} species (5).

Several research groups have claimed that the allyl-

0021-9517/94 $6.00

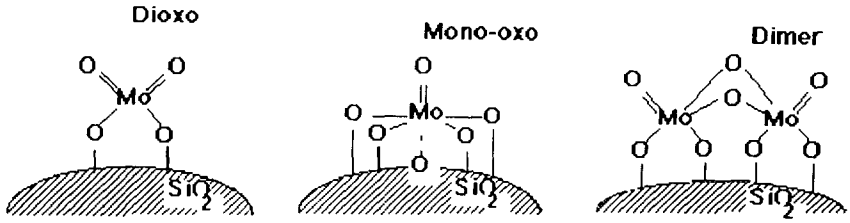

SCHEME 1

derived Mo/SiO_2 species possess unique structures which are preparation dependent. Yermakov reported that the preparation with $Mo(\eta^3C_3H_5)_4$ results in surface molybdenum oxide species bonded to the silica through two Si–O–Mo bridges (dioxo structure) (16) for the Mo(VI) oxidation state from infrared and ESR measurements. Iwasawa (12) reported that supporting $Mo(\eta^3C_3H_5)_4$ or $Mo_2(\eta^3C_3H_5)_4$ results in isolated or paired bidentate MoO_4 tetrahedra joined by bridging oxygen, respectively, as concluded from photoluminescence, DRS–UV–VIS and EXAFS studies of the dehydrated samples. Dimeric structures have also been reported by Ichikawa and co-workers (17, 18) to result from the $Mo_2(OAc)_4$ precursors based on *in situ* FTIR, DRS–UN–VIS, and EXAFS studies of the samples under oxygen and water free conditions. The allyl-derived structures were reported to be stable under repeated oxidation (673 K) and reduction (773 and 813 K) cycles (12). These structures, however, could not be reproduced by Ekerdt and co-workers (11) employing Raman spectroscopy.

The preparation of catalysts by the reaction of $MoCl_5$ with the silica surface hydroxyl groups has been proposed by Che and co-workers to present higher molybdenum oxide dispersions and better catalytic activity during methanol oxidation than catalysts prepared by impregnation with ammonium heptamolybdate (4, 15). In this preparation method, surface polymerization of the molybdenum precursor to dimeric Mo_2Cl_{10} is very important and only a very small amount is really hydrolyzed by the silanol groups. Consequently, an ammonium hydroxide washing step is required to remove the molybdenum species which have not been hydrolyzed by the silica hydroxyl groups and remain loosely bound. The ammonium hydroxide washing step, however, removes up to 90% of the molybdenum initially deposited (4). After calcination, the remaining dispersed surface molybdenum oxide species is reported to have a tetrahedral geometry with two oxo groups (dioxo structure) based on luminescence studies. Ekerdt and co-workers (11) concluded from Raman spectroscopy that surface octahedral mono-oxo molybdenum oxide species were present after such a preparation. A new procedure to obtain well-dispersed molybdenum oxide on silica, by impregnating with Mo^{3+} aqueous solutions, has been proposed by de Boer *et al.* (5). In this preparation method, Mo^{3+} interacts more strongly with silica than Mo(VI) species due to its basic properties. Oxidizing the surface Mo^{3+} species to Mo(VI) results in an isolated mono-oxo MoO_6 structure based on Raman, IR, and EXAFS/XANES characterization studies (5, 26).

The great variety of preparation methods, types of silicas, characterization methods, and activity studies employing different probe reactions results in a significant lack of homogeneity and, therefore, agreement among the various authors. The objective of this work was to systematically characterize various Mo/SiO_2 catalysts obtained from different laboratories with one characterization technique (Raman spectroscopy) and one probe reaction (methanol oxidation) in order to address the origin of these disagreements. The selective oxidation of methanol was chosen as the probe reaction because it is very sensitive to the nature of the surface sites present in oxide catalysts. Surface redox sites form primarily formaldehyde and to a lesser extent methyl formate as the reaction products. Surface acid sites result in the formation of dimethyl ether. Methyl formate results from the participation of CH_3OH adsorbed on the silica surface hydroxyl and adjacent surface molybdenum oxide sites (19). The Mo/SiO_2 samples were supplied by nine different research groups, using four different synthesis methods (grafting with washing, allyl compounds of molybdenum, impregnation with ammonium heptamolybdate, and impregnation with Mo^{3+} solutions) and up to eight different silicas (porous and nonporous with BET surface areas ranging from 20 to 400 m^2/g) as shown in Tables 1 and 2.

EXPERIMENTAL

Catalyst Preparation

The Mo/SiO_2 samples were provided by several research groups, and Tables 1 and 2 identify all the samples used with information on the preparation method and the specific silica support. The codes used to identify the different series are as follows: **I**, impregnated samples; **E**,

TABLE 1

Classification of the Silica-Supported Molybdena Catalysts Studied

	Group	Preparation[a]	Molecular Characterization: Technique	Conditions	Proposed structure	Ref.	Series code
1	Blasse	AHM	Photo luminescence	Vacuum	Dioxo	(14)	I1
2	Che[b]	Grafting	Photo luminescence ESR	Vacuum	Dioxo	(4)	G2a G2b
3	Datye	AHM	TEM	Vacuum	Dispersed	(13)	I3
4	Ekerdt	Allyl	Raman IR NMR	*In situ*	Mono-oxo	(11)	A4
	Ekerdt	Grafting	Raman IR NMR	*In situ*	Mono-oxo	(11)	G4
5	Fierro	AHM	XPS NO adsorption Raman	Ambient	Dispersed	(7)	I5
6	Geus	Mo^{3+}	EXAFS Raman IR	*In situ*	Mono-oxo	(5)	E6
7	Oyama	AHM	Raman	*In situ*	Dioxo	(20)	I7
8	Spencer	AHM				(6)	I8
9	Wachs	AHM	Raman	*In situ*	Mono-oxo	(21)	I9

[a] AHM is impregnation with aqueous solutions of $(NH_4)_2Mo_7O_{24} \cdot 4H_2O$; Grafting is by reacting $MoCl_5$ with silica silanol groups; allyl is by reaction of silica silanol groups with molybdenum ally derivatives and Mo^{3+} is impregnation of Mo^{3+} aqueous solutions.

[b] Samples from two different batches were supplied by this group and are identified as G2a and G2b.

TABLE 2

Some Characteristics of the MoO_3/SiO_2 Catalysts

Sample	Preparation method	Silica support	Calcination Temp. (K)	Silica B.E.T. Surface Area (m^2/g)	Ref.
I1	AHM impregnation	Degussa Aerosil-200	798	180	(14)
G2	$MoCl_5$	Rhône–Poulenc XOA-400	773	400	(4)
I3	AHM impregnation	Strobe	573	<20	(13)
A4	Allyl compounds	Davidson-952[a]	773	280	(11)
G4	$MoCl_5$	Davidson-952[a]	773	280	(11)
I5	AHM impregnation	Degussa Aerosil-200	873	180	(7)
E6	Mo^{3+}	Degussa Aerosil-200	723	180	(5)
I7	AHM impregnation	Cab-O-Sil		90	(20)
I8	AHM impregnation	Cab-O-Sil M5[a]	873	185	(6)
I9	AHM impregnation	Cab-O-Sil EH5	773	380	(21)

[a] Acid washed to remove impurities.

samples prepared by impregnation with electrochemically reduced molybdenum species (Mo^{3+}); **A**, samples prepared by interaction with the allyl molybdenum compound $Mo_2(\eta^3C_3H_5)_4$; and **G**, samples prepared by grafting with $MoCl_5$. The number is used to discriminate between the different research groups. Additional letters "a" or "b" identify different batches for the same method from a specific group.

Elemental Analysis

The loading of molybdenum oxide on the catalysts was determined using a Perkin–Elmer 3030 atomic absorption spectrometer. The samples were prepared by dissolving in a HF, HCl, and HNO_3 solution and were further treated in a microwave oven at a power of 650 W.

Additional XPS measurements were performed for surface chemical analysis using a Fisons ESCALAB MkII 200R spectrometer fitted with a hemispherical electron analyzer and a Mg anode X-ray exciting source (Mg$K\alpha$ = 1253.6 eV). The residual pressure in the analysis chamber was below 3×10^{-9} Torr (1 Torr = 133.3 Pa).

Laser Raman Spectroscopy

The molecular structures of the surface molybdenum oxide species on silica were examined with Raman spectroscopy. The Raman spectrometer system possessed a Spectra-Physics Ar^+ laser (Model 2020-05) tuned to the exciting line at 514.5 nm. The radiation intensity at the samples was varied from 10 to 70 mW. The scattered radiation was passed through a Spex Triplemate spectrometer (Model 1877) coupled to a Princeton Applied Research OMA III optical multichannel analyzer (Model 1463) with an intensified photodiode array cooled to 238 K. Slit widths ranged from 60 to 550 μm. The overall resolution was better than 2 cm^{-1}. For the *in situ* Raman spectra of the dehydrated samples, a pressed wafer was placed into a stationary sample holder that was installed in an *in situ* cell which has previously been described (22). Spectra were recorded in flowing oxygen at room temperature after the samples were dehydrated in flowing oxygen at 573 K. The MoO_3/SiO_2 samples had to be calcined for at least 2 h before the Raman measurements to eliminate the fluorescence from the support. Essentially the same Raman spectra were obtained with lower calcination pretreatment temperatures, but the signal to noise ratio was usually low.

In situ Raman spectroscopy during methanol oxidation was also preformed in order to study the structural changes taking place for the silica-supported molybdenum oxide catalysts. These spectra were performed with a second Raman apparatus consisting of an Ar^+ laser (Spectra Physics, Model 165), a triple grating spectrometer (Spex, Model 1877), a photodiode array detector (EG&G, Princeton Applied Research, Model 1420), and a specially designed *in situ* sample cell. The 514.5-nm line of the Ar^+ laser with 10–100 mW of power is focused on the sample disc in a right-angle scattering geometry. The *in situ* cell was equipped with a spinning sample holder which was generally rotated at ca. 1000 rpm inside a quartz cell which allows working under controlled atmosphere and temperature. Sample discs of 100–200 mg are held by the cap of the metallic alloy sample holder. A cylindrical furnace surrounding the quartz cell heats the sample and is controlled by an internal thermocouple. The MoO_3/SiO_2 samples had to be calcined at 773–973 K for at least 2 h before the Raman measurement to eliminate the fluorescence from the support. The *in situ* Raman spectra were obtained under continuous flow of a gaseous mixture with a He/O_2 ratio near 11/6. The Raman spectra of the dehydrated samples were recorded after *in situ* heating the sample at 773 K for 30 min and cooling to 503 K, which is the methanol oxidation reaction temperature. The Raman spectra under reaction conditions were collected after passing the He/O_2 mixture gas through a methanol reservoir at 273 K for at least 30 min. After the methanol oxidation reaction, the samples were reoxidized by the He/O_2 gas at 503 and 773 K for 1 h.

Methanol Oxidation

The reactivities of the different silica-supported molybdenum oxide species were probed by the methanol oxidation reaction. The reactor consisted of a 6-mm o.d. glass tube containing ca. 50 mg of catalyst which provides differential reactor conditions by keeping conversion below 10%. The catalyst was held in place by a glass-wool sandwich. The catalysts were pretreated in flowing O_2 at 573 K prior to methanol oxidation. A methanol/oxygen/helium mixture of 6/13/81 (molar ratios) at 1 atm pressure was used as the reactant gas for all the data presented in this work. Volatilization of molybdenum in the samples with high molybdenum oxide loading was observed. The analysis of the reaction products was performed with an on-line gas chromatograph (HP-5840A) containing two packed columns (Porapack R and Carbosieve SII) and two detectors (TCD and FID). The catalytic values reported here are taken after running the reaction for a few hours when steady state has essentially been reached. The reaction temperature was maintained at 503 K and the results are presented as turnover frequency (TOF), which is defined as the number of moles of methanol converted or specific product formed per mole of molybdenum atom per second. The TOF values reported are apparent TOF values since all the supported molybdenum atoms are assumed to be active in the methanol oxidation and this may not always be the case.

TABLE 3

Molybdenum Oxide Loading and Nominal Surface Molybdenum Coverage on the Specific Silica Supports

Series Code	MoO_3/SiO_2 (%)	Mo/nm^{2a}
I1	0.62	0.1
G2a	1.31	0.1
G2b	1.29	0.1
I3	0.38	2.3
A4	2.90	0.7
G4	1.31	0.2
I5	1.40	0.3
	3.70	0.8
	6.01	1.3
E6	5.40	1.0
I7	0.98	0.5
I8	2.72	0.5
I9	1.0	0.1
	3.0	0.31
	4.0	0.42

[a] The surface molybdenum loading has been calculated assuming a complete dispersion of the molybdenum oxide species on the surface of the silica support which is supported by the Raman characterization studies below.

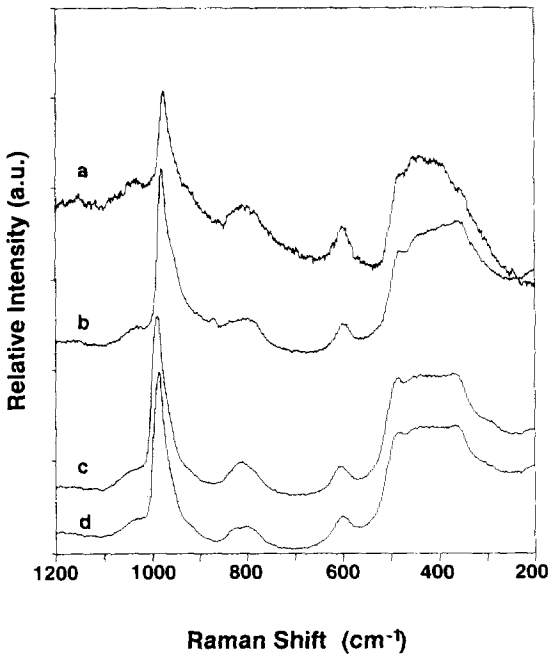

FIG. 1. *In situ* Raman spectra of dehydrated silica-supported molybdenum oxide catalysts prepared by (a) grafting on Davidson-952 silica, G4; (b) allyl derivatives on Davidson-952 silica, A4; (c) impregnation with AHM aqueous solutions on Degussa Aerosil 200 silica, I5; and (d) impregnation with Mo^{3+} solutions on Degussa Aerosil 200 silica, E6.

RESULTS

Elemental Analysis

The results of the elemental analyses of the catalysts are presented in Table 3. The molybdenum loadings are very close (typically better than 5%) to those reported by the different research groups.

Surface chemical analyses (XPS) show that most of the samples do not contain significant amount of impurities. However, the presence of alkali impurities was observed in the samples A4 (sodium) and G2b (calcium).

Laser Raman Spectroscopy

The Raman spectra of dehydrated samples prepared by impregnation with ammonium heptamolybdate (15), allylic compounds of molybdenum (A4), and grafting of $MoCl_5$(G4), impregnated with Mo^{3+} (E6) solutions, and supported on Degussa Aerosil 200, Davidson-952, Davidson-952, and Degussa Aerosil 200 silicas, respectively, are shown in Fig. 1. The broad features at 800, 650, and 500–300 cm^{-1} are due to the silica support. All the samples show the same Raman band at 978–990 cm^{-1}. Another series of Raman spectra of samples prepared by impregnation with AHM (I1, I3, I7, I8, I9) and grafting with $MoCl_5$ (G2a) and using different silica supports (Strobe, 20 m^2/g; Cab-O-Sil, 90 m^2/g; Degussa Aerosil 200, 180 m^2/g; Cab-O-sil M5, 185 m^2/g; Cab-O-Sil EH5, 380 m^2/g; and Rhône–Poulenc XOA-400, 400 m^2/g) is presented in Fig. 2. The Rhône–Poulenc sample gave a very weak Raman signal because of strong sample fluorescence. The Strobe silica presents a high number of silanol groups that result in very intense silica Raman bands at 970, 800, 600, and 485 cm^{-1} relative to the surface molybdenum species (Fig. 2a) due to its low temperature preparation. Again, the only molybdenum oxide Raman band observed is the one at ~982 cm^{-1}. Despite its very low intensity, the Raman band at 982 cm^{-1} could positively be assigned to surface molybdenum oxide species since exposure of this sample (I3) to ambient conditions resulted in the transformation of this Raman band to the Raman bands characteristic of heptamolybdate species at 965–940, 880, 380–370, and 240–210 cm^{-1}. Thus, the Raman studies reveal that the same surface molybdenum oxide species is present on all the Mo/SiO_2 samples examined and is independent of the specific silica support and the preparation method.

The presence of calcium impurities on the silica support results in the formation of new compounds ($CaMoO_4$) as seen by the presence of new Raman bands at 876, 844, 794, and 319 cm^{-1} which are not affected by hydration/dehydration processes (11). This is shown in Fig. 3 for the sample prepared on Rhône–Poulenc silica.

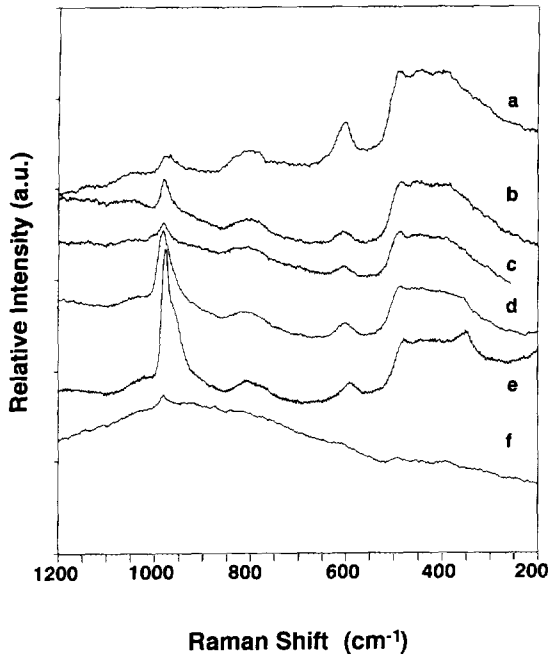

FIG. 2. *In situ* Raman spectra of dehydrated silica-supported molybdenum oxide catalysts on (a) Strobe silica, < 20 m^2/g (I3); (b) on Degussa Aerosil-200 silica, 180 m^2/g (I1); (c) on Cab-O-Sil silica, 90 m^2/g (I7); (d) on Cab-O-Sil M5 silica, 185 m^2/g (I8); (e) on Cab-O-Sil EH5 silica, 380 m^2/g (I9); and (f) on Rhône–Poulenc XOA-400 silica, 400 m^2/bg (G2a).

Along with these new Raman bands, the band characteristic of the dispersed surface molybdenum oxide species is also present at ~982 cm^{-1}.

Impregnation of silica with Mo^{3+} solutions is claimed to result in a better dispersion of surface molybdenum oxide species on the silica support. A sample prepared according to this method, shown in Fig. 4e (5), was compared with a series of molybdena/silica catalysts with higher and lower molybdenum loadings, shown in Figs. 4a–4d and 4f. This series was prepared by impregnation with ammonium heptamolybdate (7), which is reported to give the worst dispersion and the same silica support (Aerosil-200 Degussa) was employed for all the samples. The dehydrated Raman spectra of these samples are shown in Fig. 4 and the only molybdenum oxide Raman band observed is at 978–990 cm^{-1} for all the samples as well as the broad features of the silica support. At loadings close to the maximum dispersion limit of molybdenum oxide on silica (ca. 1 Mo/nm^2), a new feature can be observed at ca. 968 cm^{-1} as a shoulder. The maximum amount of Mo dispersed on SiO_2 corresponds to the titration of all the silica silanols (23). This new Raman band cannot be observed for the sample prepared from Mo^{3+} solutions, despite its high molybdenum loading. This could be indicative of a better local dispersion for the molybdenum species on this sample. In addition, preparations employing allyl molybdenum compounds also ap-

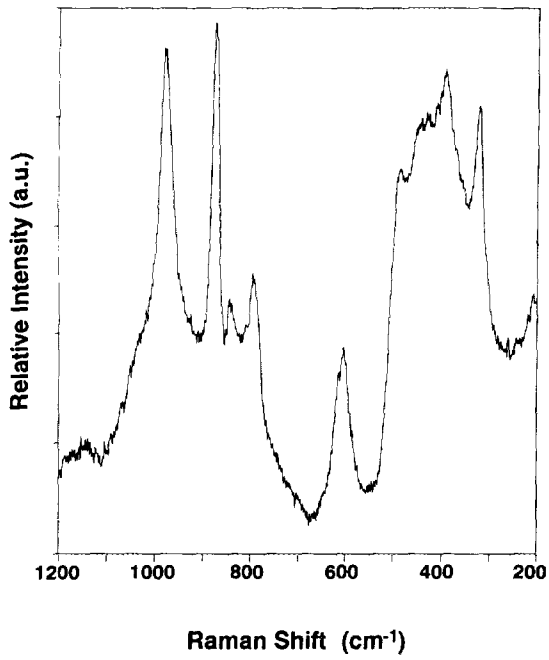

FIG. 3. Effect of calcium impurities on the molecular structures of dehydrated silica-supported surface molybdenum oxide species by means of *in situ* Raman spectroscopy of the dehydrated samples supported on Rhône–Poulenc XOA-400 silica with Ca impurities (G2b).

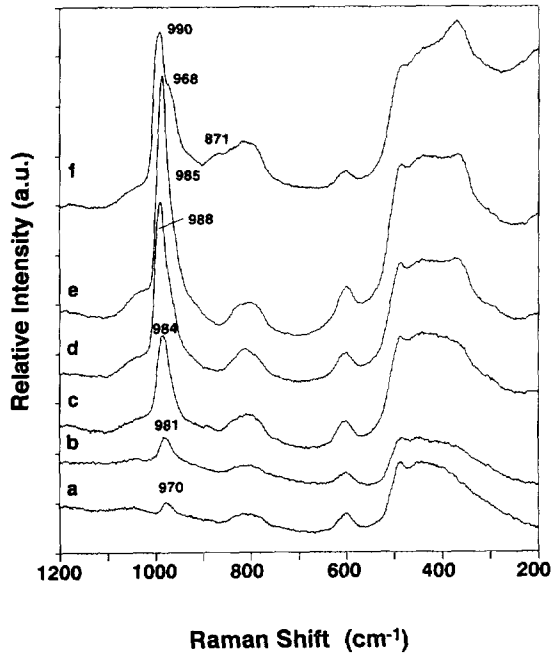

FIG. 4. *In situ* Raman spectra of the Degussa Aerosil 200 silica support and of the dehydrated silica-supported molybdenum oxide catalysts of the series I5 and E6 with surface molybdenum loadings of 0.3, 0.5, 0.8, and 1.3 Mo/nm^2 in series I5 and 1.0 Mo/nm^2 in series E6. (a) Aerosil 200; (b) 0.3I5; (c) 0.5I5; (d) 0.8I5; (e) 1.0E6; (f) 1.3I5.

pear to result in a better dispersion than observed with the conventional AHM aqueous solutions (23).

The *in situ* Raman spectra during methanol oxidation of samples prepared by impregnation with ammonium heptamolybdate (I9) and surface molybdenum loadings of 0.1, 0.3, and 0.4 Mo/nm^2 are presented in Figs. 5, 6, and 7, respectively. The broad features near 800, 600 and 500–300 cm^{-1} are due to the silica support. In addition, all the samples show the Raman band near 980 cm^{-1} under dehydrated conditions prior to exposure to the methanol oxidation reaction conditions. During methanol oxidation, the Raman band of the dispersed surface molybdenum oxide species shifts to ca. 963 cm^{-1} and, in addition, new Raman bands near 894, 842, 768, 411, 347, 305, and 279 cm^{-1} appear. The new bands become more pronounced with increasing Mo loadings. These changes in the Raman spectra occurred as soon as the catalysts were exposed to the reaction environment. The Raman spectra in Figs. 5–7 were taken after 30 min of methanol oxidation. Switching from the methanol oxidation reaction conditions to the dehydrated conditions shifts the Raman band at 963 cm^{-1} to ca. 970 cm^{-1}, but does not alter the new Raman bands near 894, 842, 768, 411, 347, 305, and 279 cm^{-1}. These new Raman bands correspond to crystalline beta-MoO_3, which is a low temperature structure of crystalline MoO_3 (40). Further treatment of beta-MoO_3 in oxygen at 773 K results in the appearance of sharp Raman bands at 991, 816, 662, 334, 284, and 150

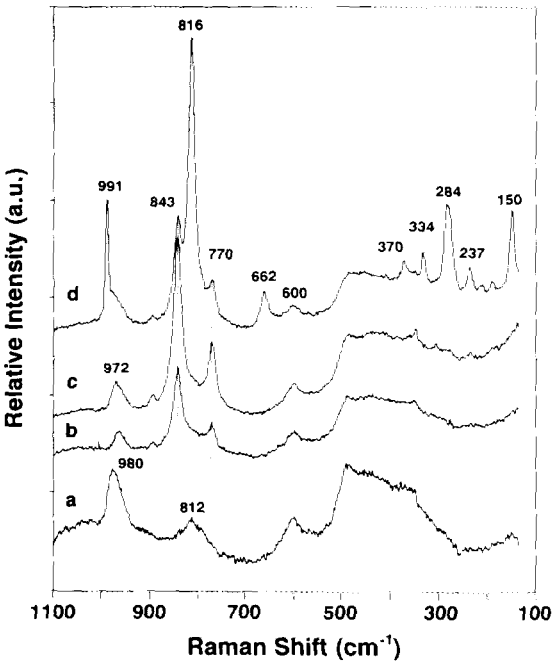

FIG. 6. *In situ* Raman spectra in reaction cell of catalyst I9 with 0.3 Mo/nm^2. (a) Dehydrated conditions, 503 K; (b) methanol oxidation at 503 K; (c) dehydrated conditions after reaction, 503 K; and (d) dehydrated after reoxidation in He/O_2 at 773 K.

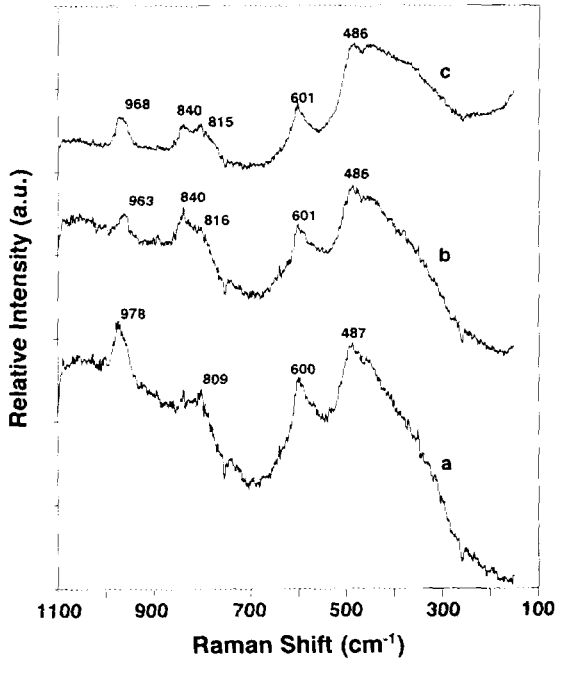

FIG. 5. *In situ* Raman spectra in reaction cell of catalysts I9 with 0.1 Mo/nm^2. (a) Dehydrated conditions, 503 K; (b) methanol oxidation at 503 K; and (c) dehydrated conditions after reaction, 503 K.

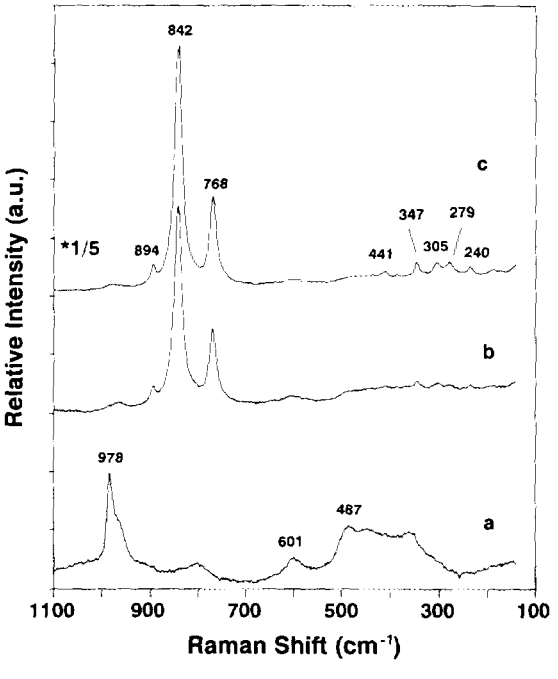

FIG. 7. *In situ* Raman specta in reaction cell of catalyst I9 with 0.4 Mo/nm^2. (a) Dehydrated conditions, 503 K; (b) methanol oxidation at 503 K; and (c) dehydrated conditions after reaciton, 503 K.

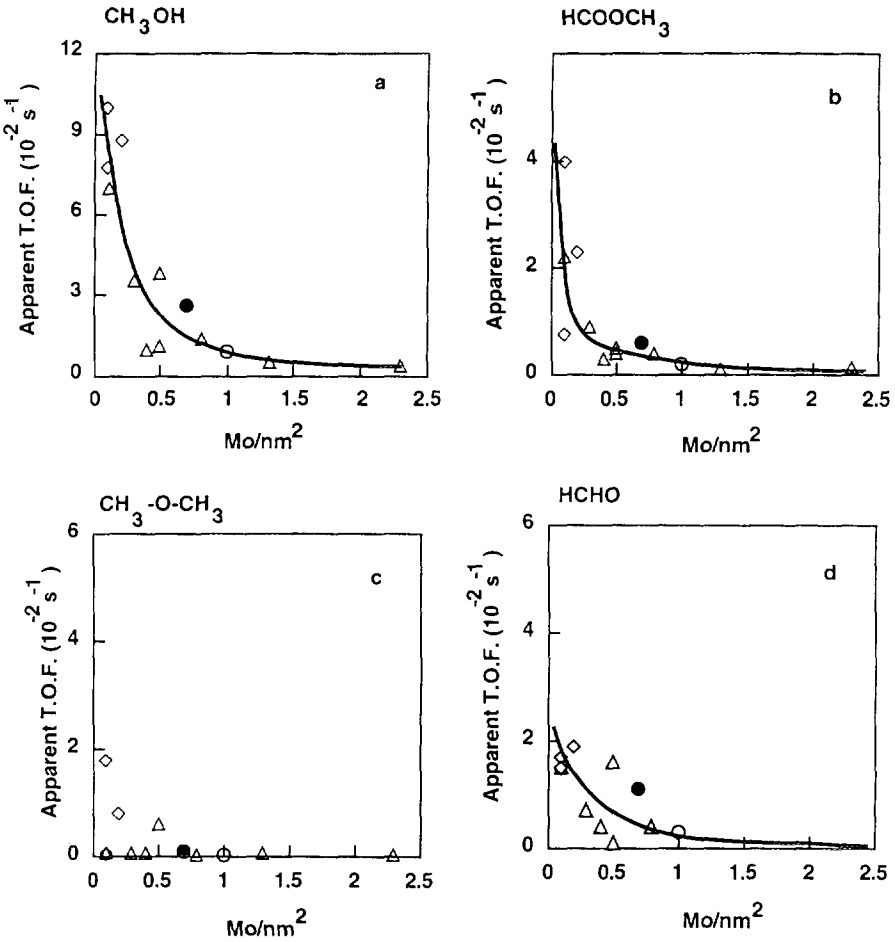

FIG. 8. Methanol oxidation on the MoO_3/SiO_2 catalysts at 503 K with a methanol/oxygen/helium feed of 6/13/81 (molar ratios) at 1 atm. Flow of 0.00035 mol-CH_3OH/h.g-cat. (a) Methanol TOF; TOF to (b) $HCOOCH_3$, (c) CH_3–O–CH_3, and (d) HCHO. (△) I-series, (◇) G-series, (○) E-series, and (●) A-series.

cm^{-1} which are due to orthorhombic crystalline alpha-MoO_3 (see Fig. 6d). Thus, the surface molybdenum oxide species on silica is not stable under methanol oxidation reaction conditions at surface densities greater than ca. 0.1 Mo/nm^2. Furthermore, even alpha-MoO_3 crystals initially present for loadings above 0.4 Mo/nm^2 are also unstable during methanol oxidation and are completely transformed to crystalline beta-MoO_3.

Methanol Oxidation

The oxidation of methanol produced mainly formaldehyde and methyl formate. Minor amounts of carbon oxides were detected, and the production of dimethyl ether remained very low for most of the samples. The results for methanol oxidation on the different Mo/SiO_2 catalysts are presented in Figs. 8a–8d as a function of the surface molybdenum oxide loading. Table 4 identifies every sample by its initial surface molybdenum coverage, preparation method, and apparent TOF in order to facilitate identification of the different samples. An increase in the molybdenum loading generally results in a significant decrease of the apparent TOF, and this is most pronounced in the case of the TOF toward methylformate. The apparent formaldehyde TOF decreases smoothly with Mo coverage and dimethyl ether production is generally low for all the molybdenum loadings studied. The dimethyl ether produced on several of the catalysts is probably the consequence of some trace acid impurities in the silica (G2a, G4, and I8). The ability to plot all the methanol oxidation catalytic data, obtained from different sources and preparation methods, essentially on a single curve as a function of Mo surface density suggests that the Mo surface coverage is the critical parameter in determining the catalytic properties of silica-supported molybdenum oxide catalysts. A similar conclusion has recently been reported by Williams and Ekerdt (24).

The catalysts show an initial transient period when the

TABLE 4

Methanol Oxidation at 503 K

Mo/nm²	Apparent TOF ($10^{-2}s^{-1}$) CH_3OH	HCHO	D.M.E.	$HCOOCH_3$	Ref.	Steady state (% dispersion)	Series code
0.1	7.8	1.7	1.8	0.75	(4)	—	G2b
0.1	10.0	1.5	0.07	4.0	(4)	100	G2a
0.1	7.0	1.5	0.05	2.2	(21)	—	I9
0.2	8.7	1.9	0.8	2.3	(11)	87	G4
0.3	3.6	0.7	0.06	0.9	(21)	36	I9
0.3	3.0	0.7	0.03	0.9	(7)	30	I5
0.4	1.0	0.4	0.6	0.3	(21)	10	I9
0.5	3.8	1.6	0.6	0.4	(6)	—	I8
0.5	1.1	0.1	0.006	0.5	(20)	38	I7
0.7	2.6	1.1	0.08	0.6	(11)	26	A4
0.8	1.4	0.4	0.03	0.4	(7)	14	I5
1.0	0.9	0.3	0.03	0.2	(5)	9	E6
1.3	0.5	0.1	0.04	0.1	(7)	5	I5
2.3	0.4	0.0	0.01	0.13	(18)	4	I3

Note. Reaction conditions: 503 K, 0.01724 mol CH_3OH/h in 50 mg catalyst.

reaction is started. During this transition period, there is a very slight increase in activity and change in the selectivities to formaldehyde and methyl formate that depends on molybdenum oxide loading. The evolution of the ratio of the apparent TOF to formaldehyde vs the apparent TOF to methyl formate for the same catalysts, which were characterized by *in situ* Raman spectroscopy during methanol oxidation, is shown in Fig. 9. The sample with the lowest surface molybdenum oxide loading (0.1 Mo/nm²) does not show any transient behavior in the selectivity. However, the catalysts with the higher molybdenum oxide loadings (0.3 and 0.4 Mo/nm²) exhibit an initial decrease in formaldehyde production and an initial increase in methylformate production.

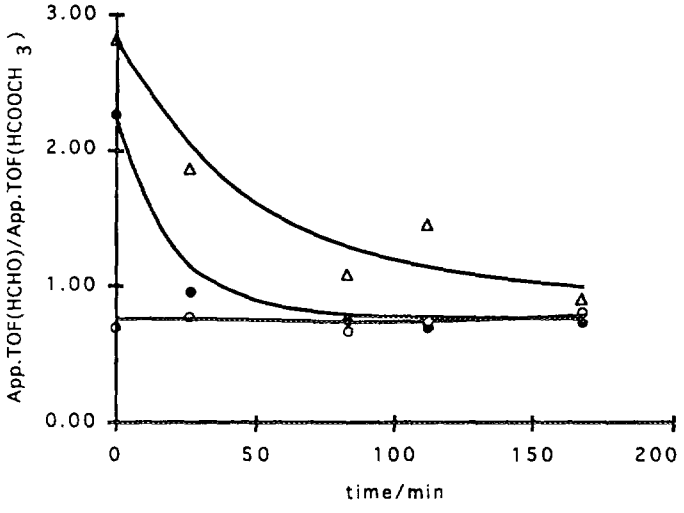

FIG. 9. Evolution of apparent TOF(HCHO)/apparent TOF($HCOOCH_3$) for catalyst I9 during the first stages of the reaction. (○) 0.1 Mo/nm², (●) 0.3 Mo/nm², and (△) 0.4 Mo/nm². Zero time corresponds to the first sample analysis which was taken after 10 min of reaction.

DISCUSSION

The Raman spectra of the dehydrated samples presented in the results section demonstrate that the preparation method as well as the specific silica support does not appear to affect the structure of the silica-supported molybdenum oxide species. Only the presence of impurities in the silica support was found to affect the nature of the surface molybdenum oxide species. The present results suggest that the apparent discrepancies in the literature between different research groups studying the MoO_3/SiO_2 system are not due to different samples, but seem to be related to the different characterization methods with regard to spectral assignments.

The isolated surface molybdenum oxide species have been reported by most authors, but there is still disagreement as to whether this species is present as mono-oxo (octahedral) or dioxo (tetrahedral). Mono-oxo MoO_6 structures have been assigned from Raman spectroscopy (5, 11, 23), IR (25, 26), and EXAFS/XANES (5). *In situ* Raman and IR studies of the same MoO_3/SiO_2 sample by de Boer *et al.* (5, 26) yield identical Mo=O vibrations at 986 cm^{-1}. This observation is significant since according to Raman/IR vibrational selection rules this coincidence should occur only for mono-oxo species (27). This conclusion is further supported by ^{18}O–^{16}O isotope experi-

ments that yield only two vibrational peaks consistent with mono-oxo species (dioxo species would be expected to yield three vibrational peaks) (25). The isolated nature of the dehydrated surface molybdenum oxide species is supported by the absence of Mo–O–Mo vibrations at 220 cm^{-1} in Raman (5, 11, 28) and the extremely low Mo–Mo coordination (SN_{Mo-Mo} = 0.30) measured by EXAFS (5, 26). The highly distorted nature of the isolated MoO_6 unit is reflected in the pre-edge feature observed in the XANES spectra and the presence of terminal Mo=O bond in Raman/IR.

The dioxo MoO_4 structures have been assigned from luminescence (29, 30), UV–visible diffuse reflectance (29), ESR (29), and Raman spectroscopy (20). Previous studies have demonstrated that UV–visible diffuse reflectance is not reliable in discriminating between MoO_4 and MoO_6 structures (11, 31). ESR can only detect Mo^{5+} species and it cannot be assumed that the same coordination is present for Mo(V) and Mo(VI) species on silica. The previous Raman spectroscopy study was reported on the same sample used in this study and the prior spectrum was not reproducible because of the adsorption of background moisture which affected the Raman features in the earlier investigation (32). In the luminescence spectra, the assignment to a tetrahedral (dioxo) structure is based on the close agreement in the emission and excitation bands with those of the MoO_4^{2-} complex in the reference compound $CaMoO_4$ (14). Calcium impurities observed in some of the samples could account for this; however, samples without $CaMoO_4$ (I1 and G2b) are also identified as dioxo by luminescence (4). Unfortunately, octahedral molybdenum species possesses such a short lifetime that it is weakly detected by luminescence (approximately ten times weaker than tetrahedral molybdenum species) (33). Consequently, luminescence can be used to detect tetrahedral molybdenum oxide species, but may not give any information on the presence or absence of octahedral molybdenum oxide species. Thus, the evidence for concluding that dioxo MoO_4 species are present on the silica surface is not very strong.

Silica-attached molybdenum dimer structures have been reported to be obtained by reacting $Mo_2(\eta^3\text{-}C_3H_6)_4$ (12, 34, 35) with the OH groups of the silica support and activating in H_2 or in an inert atmosphere (N_2). The activation of allyl dinuclear molybdenum compounds in hydrogen has been proposed to result in dimeric structures of Mo(II) based on *in situ* EXAFS measurements (34). After oxidation with molecular oxygen at 673 K, the Mo–Mo bond is not detected (34). Two different structures have been claimed for the Mo(VI) oxide surface species depending on the specific silica support (34). The silica supports employed (Snowtex-30, 120 m^2/g, SiO_2-1; and Snowtex-O, 285 m^2/g, SiO_2-2) had molybdenum loadings below 0.5 and 0.2 Mo/nm^2, respectively (35), which are well below the maximum dispersion limits of Mo/SiO_2 (~1 Mo/nm^2) and account for the homogeneity of the structures observed on each silica. On SiO_2-1, the Mo(VI) surface oxide species was reported to be tetrahedral dioxo molybdenum oxide monomers based on DRS–UV–VIS spectroscopy (band at 285 nm) of the dehydrated sample (35) and *in situ* EXAFS studies. On SiO_2-2, however, the observed DRS–UV–VIS spectrum shows a band at 306 nm characteristic of five- or six-coordinated Mo(VI) species. In addition, the XANES studies indicate that these species are highly distorted. This highly distorted structure is in agreement with the more recent XANES structures determined for samples prepared by impregnation of silica with Mo^{3+} solutions (5, 26) or by impregnation of ammonium heptamolybdate solutions (21) on a different silica (Cab-O-Sil EH5).

The presence of different molybdenum oxide structures from the same precursor on different silicas is in contrast to the current findings that the specific silica support has no effect on the structure. However, the presence of impurities, especially basic, can influence the surface molybdenum structures (36). Indeed, the presence of sodium impurities on SiO_2-1 is reported to be < 0.5% Na in a more recent work by the same authors (12). This explains the structural differences observed between the Mo(VI) species on SiO_2-1 and SiO_2-2. We have found that even very low amounts of sodium (Na/Mo = 1/15 atomic ratio) will affect the catalytic activities and surface structures of the dehydrated Mo(VI) species on silica (36). In the presence of alkali, the surface molybdenum oxide species react to form microcrystalline or molybdate phases containing tetrahedral MoO_4 species (11, 36). This effect will be even more pronounced in the case of preparations containing very low molybdenum loadings (from 0.6 to 1.5% MoO_3/SiO_2 on SiO_2-1) (35) since the Na/Mo atomic ratio varies from ~2 to 10. This high Na-to-Mo ratio accounts for the tetrahedral structure observed for molybdenum oxide on SiO_2-1.

On the sodium-free silica (SiO_2-2), no direct Mo–O–Mo bonding is observed above 200 K (dimeric surface molybdenum oxide species could be detected only at 80 K), but evidence is presented for the existence of two molybdenum oxide entities in close vicinity (12). Similar results are reported on a third silica support (SiO_2-3, 510 m^2/g) (12). This is most probably due to the dinuclear nature of the precursor which increases the probability of anchoring two Mo species in close proximity. It has recently been demonstrated with EXAFS and Raman spectroscopy that heptamolybdate clusters spread on the silica support upon dehydration resulting in dispersed, isolated mono-oxo molybdenum oxide species (5). For these samples the molybdenum anchorage to the silica surface takes place at elevated temperatures, where the silanol population is significantly decreased and prevents

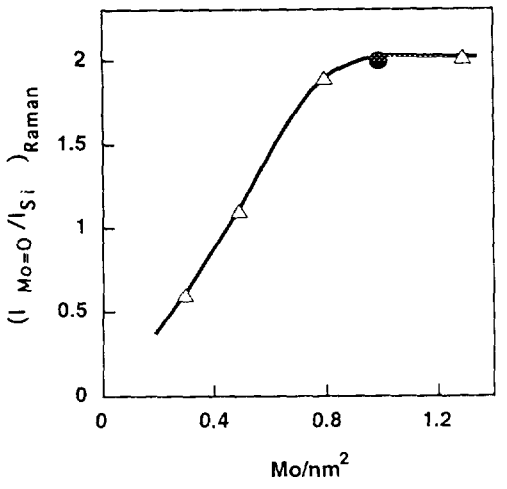

FIG. 10. Amount of dispersed surface molybdenum oxide monooxo species as a function of the Mo surface coverage on Degussa Aerosil 200 silica. (△) Series I5 and (●) serie E6.

the formation of molybdenum species in close vicinity. However, in the dimeric molybdenum–allyl samples the anchorage takes place at low temperatures and this may possibly account for their proximity with this preparation. More importantly, however, is that the XANES studies showed that the surface Mo(VI) structure on silica is the same from the allyl preparation and the samples used in the present study employing different preparation methods. The current study also found that the same surface Mo(VI) species was formed on silica from Raman spectroscopy when using the allyl preparation (Sample A4, Fig. 1). The preparation of derived dimeric molybdenum species could not be reproduced in the present study since dimeric features could not be detected in the EXAFS measurements of these samples taken by Iwasawa (51). In fact, the synthesis of this dimeric species on silica has been attempted by several different research groups and all were unsuccessful (11, 52, 53). Thus, it has been difficult to independently confirm that such a dimeric molybdenum oxide species can be formed on silica via the allyl preparation.

Formation of silicomolybdic acid in silica-supported molybdenum oxide samples has also been reported by several authors (8, 38, 44, 45). Our preliminary results show that silicomolybdic acid supported on silica is indeed formed at room temperature only after exposure to very moist air (38, 46). However, its formation requires a prolonged exposure to amounts of water larger than those present under standard ambient conditions. The silicomolybdic acid is stable at temperatures below 570 K (39) and it breaks up and spreads into isolated surface molybdenum oxide species when the temperature is higher than 570 K (38, 46). Thus, silicomolybdic acid formation requires special conditions which are usually not encountered in conventional studies and accounts for the absence of this species in most studies of the MoO_3/SiO_2 system. Actually, molybdenum oxide/silica samples prepared by Che *et al.* may have formed silicomolybdic acid during the washing step as well as samples prepared by impregnation of aqueous solutions of ammonium heptamolybdate. However, these samples are typically calcined above 570 K (see Table 2), which transforms the supported silicomolybdic acid to isolated surface molybdenum oxide species on silica.

An estimation of the degree of coverage of the surface molybdenum oxide species can be obtained from the increase in the intensity of the Mo=O Raman band at ca. 980 cm^{-1} with respect to the silica Raman band at 495 cm^{-1} since the silica band is essentially constant with molybdenum loading. This ratio is presented in Fig. 10 for the series of samples studied in Fig. 4. There is a linear increase of the Raman intensity at ~980 cm^{-1} with molybdenum loading at low coverages. The increase in the Raman intensity of the isolated surface molybdenum oxide species levels off at ca. 1 Mo/nm^2 since at this coverage there are very few available reactive silanol groups remaining which are required to stabilize the isolated surface molybdenum oxide species (2, 23). Consequently, additional isolated surface molybdenum oxide species would not be expected to form above ca. 1 Mo/nm^2 because of the unavailability of reactive silanol groups on the silica surface. A linear correlation between the molybdenum loading and the Raman shift of the Mo=O bond is also evident and is shown in Fig. 11. The Mo=O Raman band reaches a constant value of 990 cm^{-1} as a consequence of the onset of the crystalline orthorhombic MoO_3 at higher loadings. This scenario is in agreement with the appearance of a new Raman band

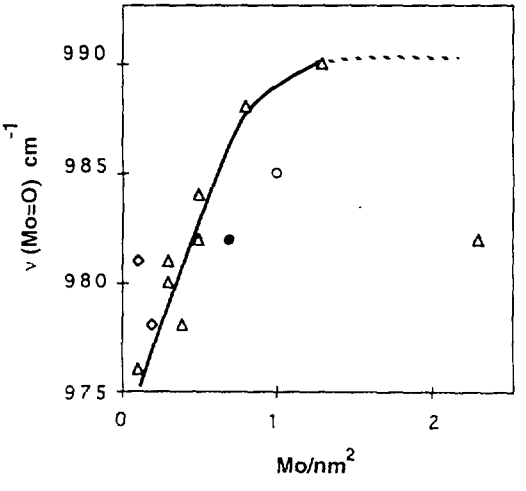

FIG. 11. Evolution of the Raman band for the Mo=O bond versus the surface molybdenum loading. (△) I-series, (◇) G-series, (○) E-series, and (●) A-series.

at ca. 968 cm^{-1} which may represent a polymerized molybdenum oxide species such as a cluster (23) that cannot spread any more and may be the precursor to the formation of larger crystalline aggregates. This new molybdenum oxide species is different from the heptamolybdate species present in the hydrated state which gives a Raman band at ~945 cm^{-1} (11). The availability of silanol groups is the determining factor for the dispersion of molybdenum oxide species on silica. The samples prepared by incorporation of Mo^{3+} and allyl derivatives exhibit a somewhat lower wavenumber for the Mo=O bond than expected for the same loading from the samples prepared by impregnation. This may be indicative of a better local dispersion for these samples with respect to those prepared by impregnation. However, the estimation of the isolated surface molybdenum oxide species from the intensity of the Raman band at ca. 980 cm^{-1} fits well with the values obtained from the samples prepared by impregnation with ammonium heptamolybdate (Fig. 10). Catalyst I3 shows a much lower wavenumber for the very high molybdenum loading and the Raman band at 968 cm^{-1} is unusually pronounced for this sample. This Raman band is associated with the silica support since hydration treatments have no effect on this Raman band. Despite its very high surface molybdenum coverage, 2.3 Mo/nm^2, no aggregated molybdenum oxide species are observed. The high dispersion on this silica is achieved because of the high number of silanol groups present in this sample which resulted from the special low-temperature silica synthesis (13). This is in agreement with the importance of availability of silanol groups in the formation of the dispersed surface molybdenum oxide species (2, 23). Consequently, the availability of reactive silanol groups for a specific molybdenum oxide loading is significantly higher for this sample than for the other silicas prepared or synthesized at elevated temperatures.

The selective oxidation of methanol on the silica-supported molybdenum oxide samples, presented in Fig. 8, shows a continuous decrease in the apparent TOF for methanol oxidation with increasing molybdenum surface coverage for all the samples studied. The decrease in methanol conversion with surface molybdenum oxide coverage is mainly due to the sharp decrease in the apparent TOFs to methyl formate formation, and the apparent TOF for HCHO shows a smoother decrease with molybdenum oxide loading. The trends presented here essentially depend only on the surface molybdenum oxide coverage, and are essentially independent of preparation method and specific SiO_2 support. The product formation trends agree with the mechanistic model proposed by Che and co-workers (4). There are two active sites in the oxidation of methanol over silica-supported catalysts: surface molybdenum oxide sites and silanol groups. Surface molybdenum oxide sites which interact with methanol form HCHO that may desorb or further interact with another methanol molecule anchored on the silanol groups of the silica surface resulting in the formation of methyl formate. The increase in the surface molybdenum coverage has a negative effect on the formation of methyl formate since the surface molybdenum oxide species aggregates to crystalline beta-MoO_3. These effects account for the significant decrease in methanol conversion to methyl formate which requires both adjacent sites. It is interesting to note that molybdena on silica samples prepared by impregnation with ammonium heptamolybdate at very low coverages results in an activity very similar to that of samples prepared by grafting at similar surface molybdenum oxide loading. The grafting method is limited by the washing step, which eliminates most of the molybdenum and prevents high molybdenum loadings (37). Consequently, the high activities reported for grafted samples toward methyl formate may be due primarily to the lower Mo loadings rather than to the preparation method. The reactivity trends observed for methanol conversion to formaldehyde also do not show any dependence on the preparation method, but also depend only on the molybdenum oxide surface coverage. The very high silanol population in sample I3 accounts for the very high selectivity to methyl formate observed (no formaldehyde is detected for this sample), according to the above mechanistic model.

The presence of basic impurities results in a lower TOF for the partial oxidation of methanol (37, 24) due to the formation of alkali molybdates (11) with different redox properties (37). In the case of the sample A4, where traces of sodium were found as impurities by XPS, no sodium molybdates were detected by Raman spectroscopy and the methanol oxidation results followed the expected trends. In sample G2b, however, Ca impurities were measurable by XPS and the presence of $CaMoO_4$ was observed by Raman spectroscopy. On the other hand, its homologue (G2a), prepared by the same group in a different batch, possessed no Ca impurities as measured by XPS, and $CaMoO_4$ was not detected by Raman spectroscopy. The absence/presence of $CaMoO_4$ in these two samples results in different catalytic properties for the selective oxidation of methanol. The Ca-free sample (G2a) exhibited a high activity to methyl formate, as already reported (2), and the activity to methyl formate was significantly decreased by the presence of calcium impurities.

The *in situ* methanol oxidation studies revealed that the surface molybdenum oxide species are not stable for catalysts containing high surface Mo densities during methanol oxidation and agglomerated to crystalline beta-MoO_3. The extent of agglomeration increased with Mo loading. When the dehydrated sample is exposed to

methanol oxidation conditions, a significant shift in the Raman band at 980 cm^{-1}, characteristic of the surface molybdenum oxide species, to ca. 963 cm^{-1} is observed. This could be due to interaction with the methoxide groups (48) which alters the length of the Mo–O bond and, therefore, its frequency (54). It is interesting to note that the Raman band at ca. 980 cm^{-1} is not affected during the selective oxidation of methane at 823 K (36), though water is formed, an no aggregation of the surface molybdenum oxide species is observed during the reaction (55). In addition, the presence of water at temperatures higher than 373 K does not affect the Raman band of the isolated surface molybdenum oxide species and no aggregation is observed (46). Thus, the interaction between the surface molybdenum oxide species and methanol must be the driving force for the aggregation into beta-MoO_3. The fact that silicomolybdic and phosphomolybdic acids are converted to beta-MoO_3 during methanol oxidation (56) provides further evidence for this model.

Another important factor associated with the aggregation of the surface molybdenum oxide species into crystalline beta-molybdena is the volatilization of the active phase. Volatilization of aggregated crystalline molybdenum oxide (alpha-molybdena) is higher than that of dispersed surface molybdenum oxide species (41, 42), and its volatilization is further promoted in the presence of water (42, 43) which is produced during the oxidation of methanol. The present work shows that increasing molybdenum loadings result in increasing degrees of aggregation of the surface molybdenum oxide species into beta-MoO_3. This behavior parallels the higher volatility observed at higher loadings of molybdenum oxide on silica.

The extent of agglomeration of surface molybdenum oxide species can be estimated from the comparison of the apparent TOFs of the surface molybdenum oxide species and beta-MoO_3. The true TOF for the dispersed surface molybdenum oxide species can be determined from the samples possessing the lowest molybdenum loadings in Table 4, 0.1 Mo/nm^2 where only a trace of beta-MoO_3 is formed (Fig. 5), and corresponds to approximately $7–10 \times 10^{-2}$ s^{-1}. The true TOF for bulk alpha-MoO_3 powder was measured and found to be approximately 2×10^{-2} s^{-1} (48); Chowdhry *et al.* (49) demonstrated that beta-MoO_3 is about 2–3 times more active than alpha-MoO_3 (49–51), which gives a TOF of $4–6 \times 10^{-2}$ s^{-1} for beta-MoO_3. The similar true TOFs for surface molybdenum oxide species on silica and beta-MoO_3 suggest that the decrease in the apparent TOF is directly due to a lower fraction of exposed molybdenum sites because of agglomeration. The estimated dispersions for the silica-supported molybdenum oxide catalysts during methanol oxidation are presented in the seventh column of Table 4. The few catalysts that produced significant amounts of DME were omitted from these calculations since this acid product is not associated with the molybdenum oxide sites. The estimated calculations suggest that the molybdenum oxide dispersion decreased from approximately 100 to ca. 4% during steady-state methanol oxidation as the Mo loading was increased. The formation of $HCOOCH_3$ for all Mo loadings suggests that either some surface molybdenum oxide species were still present or the microcrystalline beta-MoO_3 particles interacted with adjacent surface silanols since unsupported bulk MoO_3 does not produce $HCOOCH_3$. Sample 13, which possesses a high surface density of silanols, again behaved differently, yielding almost exclusively $HCOOCH_3$.

The initial methanol oxidation catalytic studies showed that the catalysts with high surface Mo densities experienced a decrease in the $H_2CO/HCOOCH_3$ selectivity ratio during the first 30 min. The corresponding *in situ* Raman studies revealed that the transformation of the surface molybdenum oxide species to microcrystalline beta-MoO_3 occurred as soon as the catalysts were exposed to the methanol/oxygen reaction environment and essentially did not significantly change with time. The decrease in initial $H_2CO/HCOOCH_3$ selectivity corresponds to an increase in the number of the surface molybdenum oxide species on the silica support. This suggests that a small amount of Mo from the beta-MoO_3 microcrystals was being redispersed via volatilization. The absence of any initial selectivity changes for the 0.1 Mo/nm^2 catalyst is consistent with this conclusion since essentially no crystalline beta-MoO_3 was formed on this catalyst and high-density Mo/SiO_2 catalysts possessing crystalline beta-MoO_3 exhibited this transient behavior. Thus, the molybdenum oxide in the MoO_3/SiO_2 catalyst can be both agglomerated and redispersed by exposure to the methanol oxidation reaction environment.

CONCLUSIONS

1. The preparation of silica-supported molybdena catalysts at low coverages by impregnation with an aqueous solution of ammonium heptamolybdate, Mo^{3+}, or grafting of $MoCl_5$ results in the same surface molybdenum oxide species.

2. The molecular structure of the surface molybdenum oxide species on silica is most likely that of an isolated, distorted mono-oxo MoO_6 species. The formation of dimeric molybdenum oxide species derived from allyl compounds is not observed.

3. The formation of new molybdenum oxide compounds on silica is due to the presence of basic impurities like calcium or sodium.

4. The selective oxidation of methanol is a sensitive

probe reaction to study silica-supported molybdenum oxide catalysts.

5. The surface molybdenum oxide coverage on silica and the availability of reactive silanol groups are the only factors affecting the nature of the surface molybdenum oxide species and the corresponding catalytic activity during methanol oxidation over the MoO_3/SiO_2 catalysts.

6. Dispersed surface molybdenum oxide species aggregate during methanol oxidation into crystalline beta-MoO_3 and the extent of agglomeration increases with surface Mo density.

7. The methanol oxidation apparent TOF decreases proportionally to the number of expose Mo sites because the true TOFs for the surface molybdenum oxide species and supported beta-MoO_3 are very similar: $7–10 \times 10^{-2}$ s^{-1} and $4–6 \times 10^{-2}$ s^{-1}, respectively.

ACKNOWLEDGMENTS

The authors gratefully acknowledge the different research groups that kindly supplied us with their silica-supported molybdenum oxide catalysts. The authors also thank Professor José Luís G. Fierro for performing the XPS analyses. M. A. Bañares thanks the Spanish Ministry of Education and Science for financial support. H. Hu acknowledges financial support from NSF Grant CTS-9006258.

REFERENCES

1. Ono, T., Anpo, M., and Kubokawa, Y., *J. Phys. Chem.* **90,** 4780 (1986).
2. Liu, T-C., Forissier, M., Coudurier, G., and Védrine, J. C., *J. Chem. Soc., Faraday Trans. 1* **85,** 1607 (1989).
3. Giordano, N., Meazzo, M., Castellan, A., Bart, J. C., and Ragaini, V., *J. Catal.* **50,** 342 (1977).
4. Louis, C., Tatibouët, J. M., and Che, M., *J. Catal.* **109,** 354 (1988).
5. de Boer, M., van Dillen, A. J., Koningsberger, D. C., Geus, J. W., Vuurman, M. A., and Wachs, I. E., *Catal. Lett.* **11,** 227 (1991).
6. Spencer, N. D., Pereira, C. J., and Grasselli, R. K., *J. Catal.* **126,** 546 (1990).
7. Bañares, M. A., Fierro, J. L. G., and Moffat, J. B., *J. Catal.* **142,** 406 (1993).
8. Barbaux, Y., Elamrani, A. R., Payen, E., Gengembre, L., Bonnelle, J. P., and Grzybowska, B., *Appl. Catal.* **44,** 117 (1988).
9. Che, M., Louis, C., and Tatibouët, J. M., *Polyhedron* **5,** 123 (1986).
10. Desikan, A. N., and Oyama, S. T., *J. Chem. Soc., Chem. Commun.* **88,** 3357 (1992).
11. Williams, C. C., Ekerdt, J. G., Jehng, J.-M., Hardcastle, F. D., Turek, A. M., and Wachs, I. E., *J. Phys. Chem.* **95,** 8781 (1991).
12. Iwasawa, Y., *Adv. Catal.* **35,** 265 (1987).
13. Srinivasan, S., and Datye, A. K., *Catal. Lett.* **15,** 155 (1992).
14. Hazenkamp, M. F., Thesis, University of Utrecht, The Netherlands, 1992.
15. Louis, C., Che, M., and Anpo, M., *J. Catal.* **141,** 453 (1993).
16. Yermakov, Y. I., *Catal. Rev.-Sci. Eng.* **13,** 77 (1976).
17. Zhuang, Q., Fukoka, A., Fujimoto, T., Tanaka, K., and Ichikawa, M., *J. Chem. Soc., Chem. Commun.* **11,** 745 (1991).
18. Ichikawa, M., Zhuang, Q., Li, G-J., Tanaka, K., Fujimoto, T., and Fukoka, K., *in* "New Frontiers in Catalysis" (L. Guczi, Ed.); *Stud. Surf. Sci. Catal.* **75(A),** 529 (1992).
19. Kim, D. S., Tatibouët, J. M., and Wachs, I. E., *J. Catal.* **136,** 209 (1992).
20. Desikan, A. N., Huang, L., Oyama, S. T., *J. Phys. Chem.* **95,** 10050 (1991).
21. Hu, H., Bare, S., and Wachs, I. E., to be published.
22. Machej, T., Haber, J., Turek, A. M., and Wachs, I. E., *Appl. Catal.* **70,** 115 (1991).
23. Roark, R. D., Kohler, S. D., Ekerdt, J. G., Kim, D. S., and Wachs, I. E., *Catal. Lett.* **16,** 77 (1992).
24. Williams, C. C., and Ekerdt, J. G., *J. Catal.* **141,** 430 (1993).
25. Cornac, M., Janin, A., and Lavalley, J. C., *Polyhedron* **5,** 183 (1986).
26. de Boer, M., Thesis, University of Utrecht, The Netherlands, 1992.
27. Cristiani, C., Forzatti, P., and Busca, G., *J. Catal.* **116,** 586 (1989).
28. Roark, R. D., Kohler, S. D., and Ekerdt, J. G., *Catal. Lett.* **16,** 71 (1992).
29. Louis, C. and Che, M., *J. Phys. Chem.* **91,** 2875 (1987).
30. Anpo, M., Kondo, M., Coluccia, S., Louis, C., and Che, M., *J. Am. Chem. Soc.* **111,** 8191 (1989).
31. Fournier, J., Louis, C., Che, M., Chaquin, P., Masure, D., *J. Catal.* **119,** 400 (1989).
32. Oyama, S. T., personal communication.
33. Wiegel, M., and Blasse, G., *J. Solid State Chem.* **99,** 388 (1992).
34. Iwasawa, Y., *in* "Tailored Metal Catalysts" (Y. Iwasawa., Ed.). Reidel, Dordrecht, 1986.
35. Iwasawa, Y., and Yamagishi, M., *J. Catal.* **82,** 373 (1983).
36. Bañares, M. A., Jones, M. D., Spencer, N. D., and Wachs, I. E., *J. Catal.* **146,** 204 (1994).
37. Louis, C., and Che, M., *J. Catal.* **135,** 156 (1992).
38. Rodrigo, L., Marcinkowska, K., Adnot, A., Roberge, P. C., Kaliaguine, S., Stencel, J. M., Makovsky, L. E., and Diehl, J. R., *J. Phys. Chem.* **90,** 2690 (1986).
39. Rocchiccioli-Deltcheff, C., Amirouche, M., Che, M., Tatibouët, J. M., and Fournier, M., *J. Catal.* **125,** 292 (1990).
40. McCarron, E. M., III, *J. Chem. Soc., Chem. Commun.*, 336 (1986).
41. Hu, H., and Wachs, I. E., unpublished results.
42. Liu, D., Zhang, L., Yang, B., and Li, J., *Appl. Catal. A* **124,** 349 (1993).
43. Leyrer, J., Mey, D., and Knözinger, H., *J. Catal.* **124,** 349 (1990).
44. Castellan, A., Bart, J. C. J., Vaghi, A., and Giordano, N., *J. Catal.* **42,** 162 (1976).
45. Kasztelan, S., Payen, E., and Moffat, J. B., *J. Catal.* **112,** 320 (1988).
46. Bañares, M. A., Hu, H., and Wachs, I. E., in preparation.
47. Kim, D. S., Wachs, I. E., and Segawa, K., submitted for publication.
48. Farneth, W. E. McCarron III, E. M., Sleight, A. W., and Staley, R. H., *Langmuir* **3,** 217 (1987).
49. Chowdhry, U., Ferreti, A., Firment, L. E., Machiels, C. J., Ohuchi, F., Sleight, A. W., and Staley, R. H., *Appl. Surf. Sci.* **19,** 360 (1984).
50. Machiels, C. J., Cheng, W. H., Chowdhry, U., Farneth, W. E., Hong, F., McCarron, E. M., and Sleight, A. W., *Appl. Catal.* **25,** 249 (1986).
51. Iwasawa, Y., personal communication.
52. Roberge, P. C., personal communication.
53. Hall, W. K., personal communication.
54. Hardcastle, F. D., and Wachs, I. E., *J. Raman Spectrosco.* **21,** 683 (1990).
55. Sun, Q., Klier, K., and Wachs, I. E., unpublished results.
56. Fournier, M., Aoussi, A., and Rocchiccioli-Deltcheff, C., *J. Chem. Soc., Chem. Commun.* **307** (1994).